CHEMPHYSCHEM

DOI: 10.1002/cphc.200700853

Fabrication and Visualization of Metal-Ion Patterns on Glass by Dip-Pen Nanolithography

Lourdes Basabe-Desmonts,[a] Chien-Ching Wu,[a, b] Kees O. van der Werf,[b] Maria Peter,[a] Martin Bennink,[b] Cees Otto,[b] Aldrik H. Velders,[a] David N. Reinhoudt,[a] Vinod Subramaniam,*[b] and Mercedes Crego-Calama*[a]

Fluorescent self-assembled monolayers (SAMs) are used as dip-pen nanolithography (DPN) substrates for the fabrication of patterns of Ca^{2+} and Cu^{2+} ions. The driving force for the transfer of these ions from an atomic force microscopy (AFM) tip to the surface is their complexation to organic ligands on the monolayer. By means of fluorescent surfaces, the patterns can be visualized under a fluorescence microscope. We use a custom-built atomic force fluorescence microscope (AFFM), a combination of atomic force and confocal fluorescence microscopes, to deposit the metal ions onto the sensing SAMs by DPN and to subsequently visualize modulations of fluorescence intensity in a sequential write–read mode.

1. Introduction

Development of new materials and patterning techniques on the micro- and nanometer scales are key issues in nanotechnology and fabrication of miniaturized devices.[1] Dip-pen nanolithography (DPN) is a high-resolution patterning technique that enables the preparation and registration of patterns on the length scale ranging from less than 100 nm to many micrometers.[2,3] Ink molecules are transported from the tip to a substrate when the tip is in contact with the surface of the substrate.[2,4] The driving force for this transport can be chemical[5] or electrochemical.[6] Dip-pen nanolithography has several advantages over other patterning techniques such as microcontact printing (μCP).[7] Chemical arrays are obtained by surface modification with different inks by direct-write DPN,[8,9] whereas simple μCP is normally a single-ink process.[10] Moreover, the flexibility and relatively high throughput of DPN allows the preparation of a large number of different patterns on one or more different substrates.[11] DPN can be carried out as a serial process,[2,3] and an array of parallel-probe cantilevers has already been reported.[11]

Since its invention,[12] DPN has been performed with a large variety of inks such as alkyl thiols,[13] proteins,[14] DNA,[15] metal oxides,[16] organic dyes,[17,18] and other molecules[2,19–22] on gold, glass, and silicon oxide surfaces. Metal salts have been deposited on semiconductor substrates to generate metallic patterns,[23,6,24] but, to the best of our knowledge, metal ions have never been deposited on glass by DPN. This approach would enable applications such as selective and controlled immobilization of proteins by means of specific metal–protein interactions,[11,25,26] generation of metallic nanopatterns on reduction of metal-ion patterns,[27] and controlled material synthesis and crystal nucleation.[28]

The fluorescent SAMs developed by us offer a simple and efficient method for sensing metal ions by observing the modulation of fluorescence intensity.[29–31] Fluorescent self-assembled monolayers [SAM(F*x*,L*y*), see Figure 1a] are created by sequential deposition of fluorophores F*x* ($x=1, 2, 3,\ldots, n$) and ligand molecules L*y* ($y=1, 2, 3,\ldots, n$) onto amino-terminated monolayers on glass.[29] By taking advantage of the interaction of organic ligands with metal ions, these SAM-functionalized glass slides become metal-ion sensing platforms. Modulation of the fluorescence properties, that is, different degrees of fluorescence enhancement or quenching, occurs on complexation of metal ions M*z* ($z=1, 2, 3,\ldots, n$) by the organic monolayers on top of the glass slide. The use of different pairs of fluorophores and ligands leads to the fabrication of libraries of substrates SAM(F*x*,L*y*), each with different binding and ion-sensing properties.[31,32]

Together with patterning techniques, this approach yields combinatorial libraries in which each pattern P(F*x*,L*y*,M*z*) is the

[a] *Dr. L. Basabe-Desmonts,[++#] C.-C. Wu,[#] Dr. M. Peter, Dr. A. H. Velders, Prof Dr. D. N. Reinhoudt, Dr. M. Crego-Calama[+]*
Laboratory of Supramolecular Chemistry and Technology
MESA[+] Institute for Nanotechnology and Faculty of Science and Technology
University of Twente, 7500 AE Enschede (Netherlands)
Fax: (+31) 53 489 4645
E-mail: mercedes.cregocalama@imec-nl.nl

[b] *C.-C. Wu,[#] K. O. van der Werf, Dr. M. Bennink, Dr. C. Otto, Prof. Dr. V. Subramaniam*
Biophysical Engineering Group
MESA[+] Institute for Nanotechnology and Faculty of Science and Technology
University of Twente, 7500 AE Enschede (Netherlands)
Fax: (+31) 53 489 1105
E-mail: v.subramaniam@tnw.utwente.nl

[+] *Current address:*
Stichting IMEC Nederland/Holst Centre
PO Box 8550, 5605 KN, Eindhoven (Netherlands)

[++] *Current address:*
Biomedical Diagnostics Institute
Dublin City University, Collins Avenue, Glasnevin, Dublin 9 (Ireland)

[#] *These authors contributed equally to this work.*

Supporting information for this article is available on the WWW under http://dx.doi.org/10.1002/cphc.200700853.

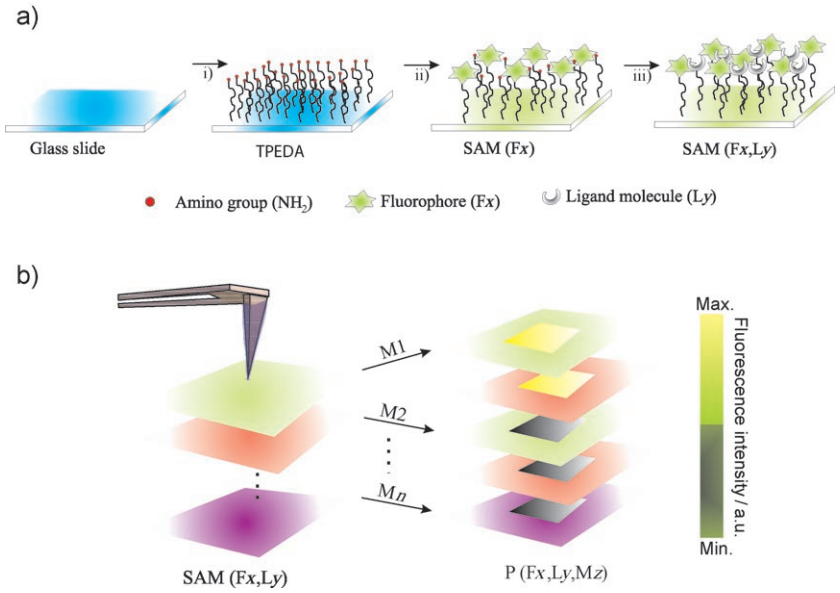

Figure 1. Schematic of a) the fabrication of a fluorescent SAM on glass [SAM(F*x*,L*y*)]: i) silanation of the glass slide with *N*-[3-(trimethoxysilyl)propyl]ethylenediamine to form the amino-terminated monolayer TPEDA, ii) reaction with an amino-reactive fluorophore F*x*, iii) covalent attachment of a ligand molecule L*y*. b) Transfer of metal ions M*z* from an AFM tip onto different fluorescent SAM(F*x*,L*y*) to form fluorescent and metal-ion patterns P(F*x*,L*y*,M*z*).

result of the combination of the three building blocks, that is, a fluorophore, a ligand , and a metal ion (Figure 1). We have previously demonstrated the fabrication of metal-ion patterns on fluorescent SAM-coated glass slides using μCP, whereby the sensing properties of the fluorescent substrates allowed visualization of the pattern by fluorescence microscopy.[30] Herein we demonstrate the controlled delivery of metal ions in well-defined micrometer and submicrometer patterns to discrete areas of the SAM-functionalized glass substrates by DPN (Figure 1).[29,31,32] The transfer of metal ions from an AFM tip to the glass surface in local areas is accompanied by selective modulation of the fluorescence of the substrate in the written areas.[30] Metal-ion and fluorescent patterns are therefore simultaneously generated on the substrates (Figure 1 b).

In addition to the novel generation of metal-ion patterns on SAM-functionalized glass by DPN, the innovative combination of atomic force microscopy (AFM) and confocal fluorescence microscopy (CLSM) for in situ fabrication and visualization of the metal ion patterns is reported.

2. Results and Discussion

2.1. DPN and Visualization with AFM and CLSM

For proof of concept, two different metal salts, $Ca(ClO_4)_2$ and $Cu(ClO_4)_2$, are patterned on two different fluorescent SAMs (TMH and TB, depicted in Figure 7). Each metal ion induces a distinct response from the fluorescent surfaces. When Ca^{2+} is complexed on the organic monolayer an enhancement of the fluorescent signal is normally observed, whereas complexation of Cu^{2+} ions induces quenching of the fluorescence emission from the monolayer.[29,30] The substrates chosen for the experiments were selected from a library of fluorescent SAMs, reported previously, based on their high sensitivity for calcium and copper ions.[29]

To carry out the writing experiments, AFM tips, immersed for 10 min in a solution of $Cu(ClO_4)_2$ or $Ca(ClO_4)_2$ (10^{-2} M, acetonitrile or ethanol) and then dried, are used to scan square areas of 20×20 μm on a glass substrate functionalized with the corresponding fluorescent SAM. The resulting patterns were immediately imaged by AFM and subsequently transferred to a confocal laser scanning microscope (CLSM) for fluorescence imaging (Figure 2). For AFM imaging of the written area, a larger area of 40×40 μm is scanned without withdrawing the tip. Height and friction images are obtained simultaneously. The AFM height images do not show any features corresponding to the written area, that is, neither mechanical deformation of the SAM nor material removal occurs (Figures 2 a, d, g, and j).

The AFM friction image of the pattern written on a TMH substrate with an acetonitrile solution of $Cu(ClO_4)_2$ as ink (Figure 2 b) shows a brighter square in the middle of the image corresponding to the area where the metal ions are deposited. A CLSM image of the surface shows a 20×20 μm pattern where the initial fluorescence of the TMH SAM is quenched (Figure 2 c), indicative of transfer of the Cu^{2+} salt from the AFM tip to the substrate. When $Ca(ClO_4)_2$ is used as ink on a TMH substrate, a bright fluorescent square feature is observed in the CLSM image consistent with transfer of Ca^{2+} ions from the AFM tip to the substrate (Figure 2 f). A 40×40 μm pattern observed in the fluorescence image corresponds to the size of the final AFM image (40×40 μm) and not to the size of the written area (20×20 μm), presumably because the same AFM tip was used to write and image the pattern. The residual ink on the AFM tip could cause further ink transfer. This observation is confirmed by the average fluorescence intensity profile of the defined area in Figure 2 f, which exhibits a larger fluorescence enhancement in the central 20 μm of the profile corresponding to the written area. The same experiment was done on the TMH substrate with $Ca(ClO_4)_2$ and EtOH instead of acetonitrile as solvent. The transfer of Ca^{2+} ions to the substrate is demonstrated by enhancement of the fluorescence intensity in the written area (Figure 2 i). Ca^{2+} ions ($Ca(ClO_4)_2$, 10^{-2} M, acetonitrile) are also deposited on TB substrates (Figures 2 j–l). In this case the friction AFM image shows a slight contrast in the written area, and an enhanced fluorescence pattern is observed in the CLSM image (Figure 2 l). Even though a 40×40 μm pattern cannot be observed easily in panels c, i, and l, the average fluorescence line intensity profiles across

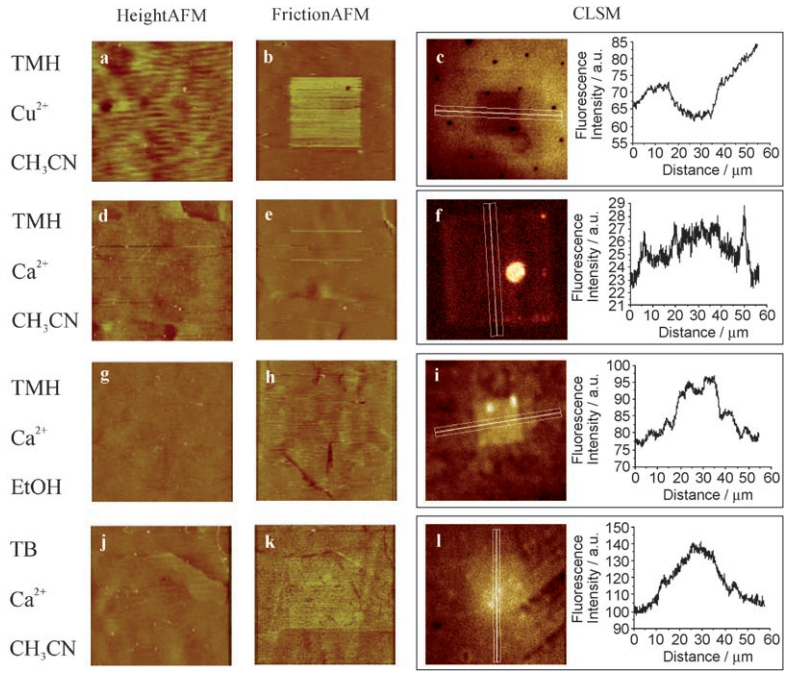

Figure 2. Friction and height AFM images (40×40 μm) and CLSM images (60×60 μm) of the fluorescent TMH monolayers (images a–i) in which 20×20 μm metal-ion patterns were written by DPN. TMH SAMs were patterned with Cu^{2+} [Cu $(ClO_4)_2$, 10^{-2} M, acetonitrile; images a–c], with Ca^{2+} [Ca $(ClO_4)_2$, 10^{-2} M, acetonitrile; images d–f], or EtOH (images g–i). TB SAMs were patterned with Ca^{2+} [Ca $(ClO_4)_2$, 10^{-2} M, acetonitrile; images j–l]. Average fluorescence intensity profiles of the area defined by the white lines in images c, f, i, and l are also shown.

We explore other applications of these fluorescent substrates such as studying ink diffusion on the substrate and possible quantification of the transferred material. Therefore, a cross-shaped pattern was generated on the TMH substrate. Two mutually perpendicular rectangles, 60 μm long and 1.87 μm wide, were written with an AFM tip loaded with a Cu^{2+} ink ($Cu(ClO_4)_2$, 10^{-2} M, acetonitrile). The CLSM images show two fluorescence-quenched areas corresponding to the scanned areas in the AFM image (Figure 3). In the CLSM image, widths of about 6.6 μm and about 1.4 μm for the first and second written rectangles are observed, respectively. In the AFM friction image only one line, 1.95 μm wide, corresponding to the first written rectangle is observed. The second rectangle is invisible even though these images shows a similar effect to that observed in panel f. Replacement of the ink-treated tip with a new tip would avoid depositing residual ink onto the surface while obtaining the height and friction. The DPN-written area could be relocated by using fiducial markers incorporated on the substrate. However, it is not practical to change tips in our current AFM setup due to the difficulty of relocating the original written area. The transfer of metal ions to the substrates could not be detected in the AFM height images, and it is only observed for a few cases in the AFM friction images. Conversely, the fluorescent images show the presence of metal ions on the substrates. These observations indicate a lower sensitivity of AFM compared to fluorescence microscopy for the detection of metal ions patterned on fluorescent SAMs.

The absence of contrast in the AFM height image can be attributed to complexation of the metal ions within the organic SAM with insignificant consequences for the topography. We speculate that differences in the friction images are related to differences in reorganization of the fluorophores and ligands in the respective layers on metal-ion complexation. The details of the complexes of metal ions and monolayers are not fully understood yet. This current work does not aim to study the details of complex formation.

The results presented above (Figure 2) demonstrate the successful generation of Cu^{2+} and Ca^{2+} patterns on the SAM-functionalized glass surfaces by DPN, and the sensitive detection by fluorescence microscopy of small quantities of metal ions on special fluorescent SAMs.

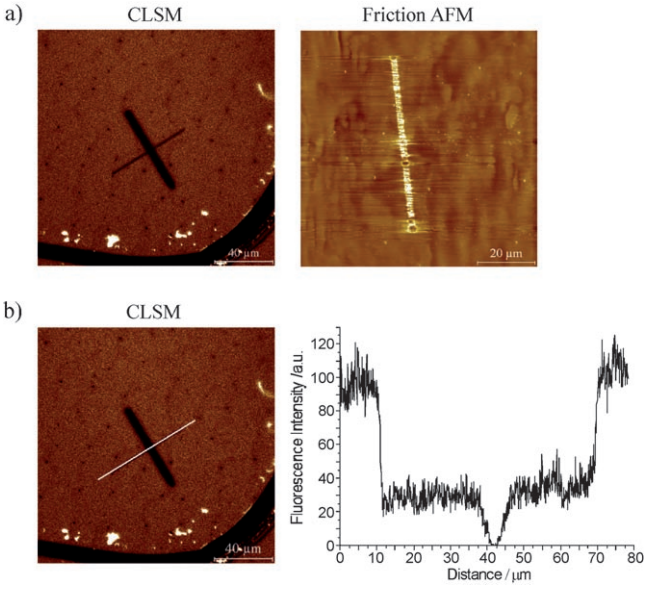

Figure 3. a) CLSM image and friction AFM images of a fluorescent TMH monolayer in which a cross-shaped pattern of two lines (60×1.87 μm) has been generated by DPN with an AFM tip inked with Cu^{2+} [$Cu(ClO_4)_2$, 10^{-2} M, acetonitrile]. b) Average fluorescence intensity profile (right) along the white line overlying the thinner DPN written line in (a).

transfer of Cu^{2+} ions to the substrate in that area is confirmed by fluorescence microscopy. The images suggest that major deposition takes place during the scan of the first rectangle which results in a shortage of ink on the tip for the second rec-

tangle. Additionally, the fluorescence images reveal that the diffusion of the ink on the substrate is much larger than observed in the AFM images. Depending on the imaging technique a difference of about 4 μm is observed for the width of the first written line. This difference is more than twice the size of the programmed line width. Presumably, due to diffusion processes, a gradient exists from a high concentration in the center towards the borders of the rectangle. Therefore, only the central part with higher concentration of Cu^{2+} is visible in the AFM images. Far from the center the concentration of Cu^{2+} is lower and is revealed only in the CLSM images.

Inspection of the fluorescence intensity profile (Figure 3b) along the second scanned rectangle shows that the fluorescence intensity in the cross intersection (ca. 41 μm) has more pronounced quenching of the initial fluorescence intensity corresponding to a higher concentration of Cu^{2+} ions in that area. This phenomenon suggests that quantitative data about the transfer of material from an AFM tip to a substrate could be extracted by evaluating the amplitude of the fluorescence intensity. The differential fluorescence quenching as a result of varying amount of ion deposition is observed also in the fabrication of Ca^{2+} patterns performed in an atomic force fluorescence microscope (AFFM).

2.2. DPN and Visualization with AFFM

Due to the intrinsic difficulty of finding the written pattern after transferring the sample from the AFM to the confocal fluorescence microscope, we are limited to using patterns with large feature sizes (20 μm or larger). To facilitate scaling down the size of the metal-ion patterns and to have better control of pattern fabrication and visualization, we performed DPN and immediate fluorescent imaging on an atomic force fluorescence microscope (AFFM).[33] Figure 4 depicts how we performed writing and visualization in situ. An AFM tip was brought into contact with a substrate right above the focus of the objective lens.

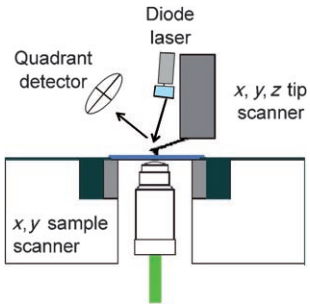

Figure 4. Schematic of DPN and in situ fluorescence visualization by AFFM.

Sequential AFFM write–read experiments confirmed an increase in fluorescence on complexation of Ca^{2+} ions to the TMH substrate. Figure 5 shows a 15×15 μm square written with Ca^{2+} ($Ca(ClO_4)_2$, 10^{-1} M, ethanol). The bright square in the fluorescence image indicates transfer of the metal ions onto

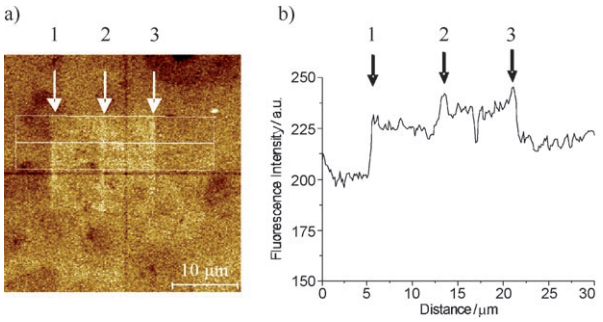

Figure 5. a) Fluorescence image of a TMH substrate obtained by AFFM. A square pattern (15×15 μm) was generated by DPN with an AFM tip inked with Ca^{2+} [$Ca(ClO_4)_2$, 10^{-1} M, ethanol]. b) Average fluorescence intensity profile of the area defined by the white lines. The arrows indicate the lines with higher fluorescence intensity.

the written area. The brighter vertical edges and central part of the square suggest (as in the case of Cu^{2+} in Figure 3) that larger amounts of metal ions were transferred from the tip onto the fluorescent SAM at these specific locations. This is in agreement with the fact that the tip is in contact with the substrate for longer times in these areas. The central part corresponds to the initial scanning process which was performed before writing the whole square pattern in order to adjust the electronic offset signal to the tilt of the substrate. During this adjustment the Ca^{2+}-loaded tip scans the same line several times. The tip was also longer in contact with the substrate at the vertical edges of the square due to the change of direction between trace and retrace at the end of each scan line. The darker cross lines shown in Figure 5 result from photobleaching of the substrate by scanning with 488 nm argon laser light before performing DPN.

We also explore fabrication and visualization of submicrometer-scale metal ion patterns on SAM-functionalized glass by DPN using an AFFM. For this purpose, $Ca(ClO_4)_2$-loaded tips are used to write lines on TMH substrates. Single lines of Ca^{2+} ions are deposited onto the substrates, and therefore bright lines with submicrometer widths are expected in the fluorescence images. During the experiments, the scan speed is varied to observe the relation between the tip–substrate contact time and the level of modulation of fluorescence. A slower speed (longer contact time between the tip and the substrate in a certain area) results in larger amounts of ink molecules being transferred to the substrate and therefore greater enhancement of fluorescence. Patterns with line widths of about 0.8 μm and 0.6 μm on a TMH substrate are presented in Figure 6a; six horizontal lines of 18 μm in length are written with six different scan speeds varying between 18 and 1.8 μm s^{-1} without retracting the tip during the whole DPN process. Each line is scanned 15 times and the fluorescence image is recorded immediately after completion of DPN of all six lines. As expected, slight differences in the brightness of the lines are observed (Figure 6a). Lines written at a lower scan rate show higher fluorescence intensity, which is in agreement with a larger amount of transferred Ca^{2+} ions. Close inspection of the profile (Figure 6b) shows a gradual increase of signal with de-

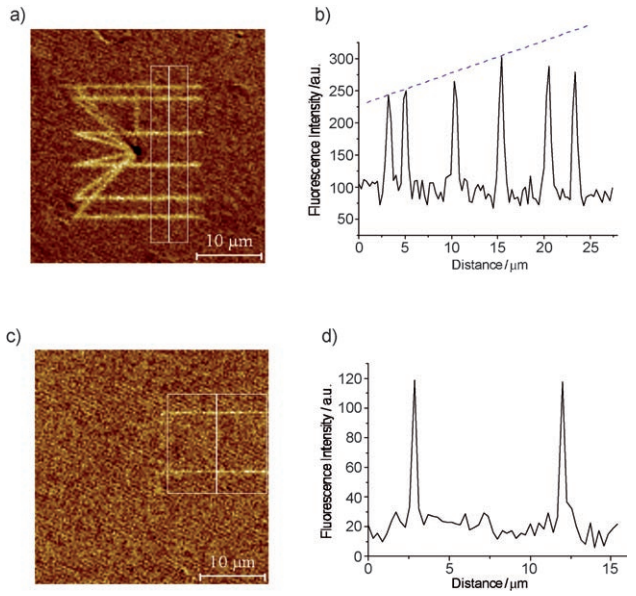

Figure 6. a) Fluorescence image of a TMH substrate acquired immediately after DPN with the AFFM. Six horizontal lines (18 μm in length) were successively generated by using an AFM tip inked with Ca^{2+} [$Ca(ClO_4)_2$, 10^{-1} M, ethanol] at scanning speeds of 17.7, 14.1, 10.6, 7.1, 3.5, and 1.8 μm s^{-1} (from top to bottom). b) Average fluorescence intensity profile of the area inside the rectangle indicated in (a). The peaks from left to right correspond to the written lines from top to bottom. The dashed line indicates the trend of increasing enhancement of fluorescence corresponding to a lower scanning speed. c) Fluorescent image of a TMH substrate acquired with the AFFM. Two horizontal lines (18 μm long) were generated by DPN using an AFM tip inked with Ca^{2+} [$Ca(ClO_4)_2$, 10^{-1} M, ethanol] for 5 (top) and 10 min (bottom). The upper line was written first. d) Average fluorescence intensity profile of the area defined by the white lines. The left peak corresponds to the upper written line. In both images (a and c), the background, that is, the fluorescence image before DPN, is subtracted.

creasing scan rate, but this trend is reversed in the last two lines. We attribute this effect to depletion of ink from the tip. Figure 6c shows two lines written with a scan rate of about 1.8 μm s^{-1} for 5 and 10 min. In spite of the fact that one line is written for a longer time, the amplitude of the fluorescence emission from both lines is the same. We postulate that, after scanning for a few minutes, the surface is saturated with Ca^{2+} ions and the maximum possible emission intensity is observed. The variations of line width between different experiments may result from a different relative humidity (RH) in the environment of the cantilever,[34] or manufacturing differences of the tip. These effects have been already reported in the literature.[2,35,36] Since ink depletion and imperfect control of ink delivery coupled with defects in the fluorescent SAMs yield inhomogeneities in the DPN-written metal-ion patterns, alternative approaches such as fountain-pen nanolithography are suitable for future experiments.[37–41]

3. Conclusions

We demonstrate that it is possible to fabricate metal-ion patterns at micrometer and submicrometer scale on nonconductive fluorescent SAM-functionalized glass substrates by dip-pen nanolithography. The driving force for the transfer of material from the AFM tip to the substrate is the formation of metal-ion complexes on the organic monolayer on the glass substrate. Such transfer of metal ions was revealed by a change in the fluorescence response of the substrate. The fluorescent SAM-coated glass substrates used for the deposition offer a number of advantages, including optical visualization of the pattern even in cases in which the concentration of metal ions on the surface is so low that the AFM images do not exhibit any feature. Moreover, the combination of the topographic resolution of the AFM and the single-molecule sensitivity of the confocal fluorescence microscope in the AFFM enhances the possibilities of this approach by allowing immediate fluorescence imaging of the fabricated patterns in a sequential write–read mode in situ. Extension of this approach to a direct write-read mode, in which the optical signal is measured simultaneously while writing with the AFM tip, has significant potential. These special substrates combined with the DPN-AFFM technique are potentially useful for the observation of ink diffusion in DPN processes.[42] Additionally, the fabrication of metal-ion patterns by DPN can be used for the production of protein nanopatterns. We are currently investigating the complexation of proteins to the metal-ion patterns created by DPN on glass substrates.

Experimental Section

General Procedures: All glassware used to prepare the layers was cleaned by sonicating for 15 min in a 2% v/v Hellmanex II solution in distilled water, rinsed four times with high-purity water (MilliQ, 18.2 MΩ cm), and dried in an oven at 150 °C. Microscope glass slide substrates were cleaned for 15 min in piranha solution (concentrated H_2SO_4 and 33% aqueous H_2O_2 in 3:1 ratio). Warning: Piranha solution should be handled with caution. It has been reported to detonate unexpectedly. They were then rinsed several times with high-purity water (MilliQ), and dried in a nitrogen stream immediately prior to formation of the monolayer.

Monolayer Preparation:[29] The amino-terminated self-assembled monolayer was prepared in a glove box under an atmosphere of dry nitrogen. Freshly cleaned substrates were immersed in a 5 mM solution of *N*-[3-(trimethoxysilyl)propyl]ethylenediamine (TPEDA) in dry toluene (freshly distilled over sodium) for 3.5 h. After the substrates were removed from the solution, they were rinsed twice with toluene (under nitrogen atmosphere) to remove excess silane and avoid polymerization. The substrates were then removed from the glove box and rinsed with ethanol and dichloromethane to remove physisorbed material. The following protocol was repeated twice: shaking of the slide in a beaker filled with EtOH, then rinsing with a stream of EtOH, followed by stirring in CH_2Cl_2, then rinsing with a stream of CH_2Cl_2. The slides were then dried under an air stream.

For synthesis of the TM and T SAMs, the fluorophores were attached to the TPEDA SAM by immersing the slide for 4 h in an Erlenmeyer flask with 50 mL of a 0.23 mM acetonitrile solution of the fluorophore TAMRA [5(6)-carboxytetramethylrhodamine, succinimidyl ester = 5(6)-TAMRA, SE (mixture of isomers)] or fluorophore TRITC (tetramethylrhodamine-5(6)-isothiocyanate = 5(6)-TRITC (mixture of isomers)] to yield TM and T, respectively. Then the substrates were removed from the solution and rinsed with CH_3CN, EtOH, and CH_2Cl_2 to remove physisorbed material. The slides were

then dried under an air stream. For the synthesis of the TMH SAM, the TM-functionalized slides were immersed in CH_3CN solution of hexanoyl chloride (50 mM) to afford TMH. Et_3N (100 μL) was added to the hexanoyl chloride solution. For the synthesis of TB, the T-functionalized slides were immersed in a CH_3CN solution of benzoyl chloride (50 mM). Et_3N (100 μL) was added to the solution. All reactions were carried out under an atmosphere of dry N_2 for 16 h. After the substrates were removed from the solution, they were rinsed sequentially with CH_3CN, EtOH, and CH_2Cl_2 to remove physisorbed material. The slides were then dried under an air stream. All glass slides functionalized with fluorescent SAMs (TM, TMH, T, and TB) were then sonicated for 1 min in a beaker filled with CH_2Cl_2, rinsed again with CH_2Cl_2, and dried under an air stream to assure a clean fluorescent monolayer. The synthetic scheme of SAM fabrication is shown in Figure 7. SAM formation on the glass slides was characterized by ellipsometry, water contact-angle goniometry, fluorescent spectroscopy, and XPS, as reported elsewhere.[29]

By using the fluorescent SAMs prepared by following the original protocol,[29] we found that the fluorescence emission could be enhanced simply by scanning with 488 nm argon laser light. We conjectured that the high concentration of fluorophores on top of the SAM results in a self-quenching process. By scanning with the laser light, some fluorophores were inactivated by photobleaching, which resulted in reduced self-quenching and thus fluorescence enhancement. To avoid any potential influence of self-quenching on analyses of DPN results, the original protocol for preparing sensing SAMs was modified to use significantly lower fluorophore concentrations. TM SAMs prepared in different fluorophore concentrations for 2 h were examined for fluorescence enhancement caused by laser scanning. Furthermore, all of the TM SAMs were microcontact-printed with metal ions to determine whether they retained the ability to sense metal ions. Based on these results, a TAMRA solution of 0.01 mM was chosen to prepare fluorescent SAMs for systematic dip-pen nanolithography experiments by AFFM. For details, see the Supporting Information.

Dip-Pen Nanolithography with Metal-Ion Solutions on TMH and TB: Initially, the dip-pen nanolithography experiments were performed on a Nanoscope III Atomic Force Microscope (AFM) (Veeco-Digital Instruments) operated under ambient conditions in contact mode. The AFM was equipped with a J scanner. Commercial Si_3N_4 cantilevers were used with a nominal spring constant of 0.58 $N\,m^{-1}$. Prior to writing, the tips were immersed in a 10^{-2} M acetonitrile or ethanol solution of the perchlorate salts of Cu^{2+} or Ca^{2+} for 10 min and dried in air. For writing square-shaped patterns in DPN experiments, an area of 20×20 μm was scanned for 30 min using a scan rate of 1 Hz (40 $\mu m\,s^{-1}$). The load applied by the tip to the sample was kept between 5 and 15 nN. The relative humidity of the air was between 48 and 55%, and the temperature between 25 and 28 °C. The maximum heights shown in Figures 2a, g, j and Figure 2d are 20 and 10 nm, respectively; the maximum friction voltages shown in Figures 2b, h, k and Figure 2e are 0.15 and 0.2 V, respectively.

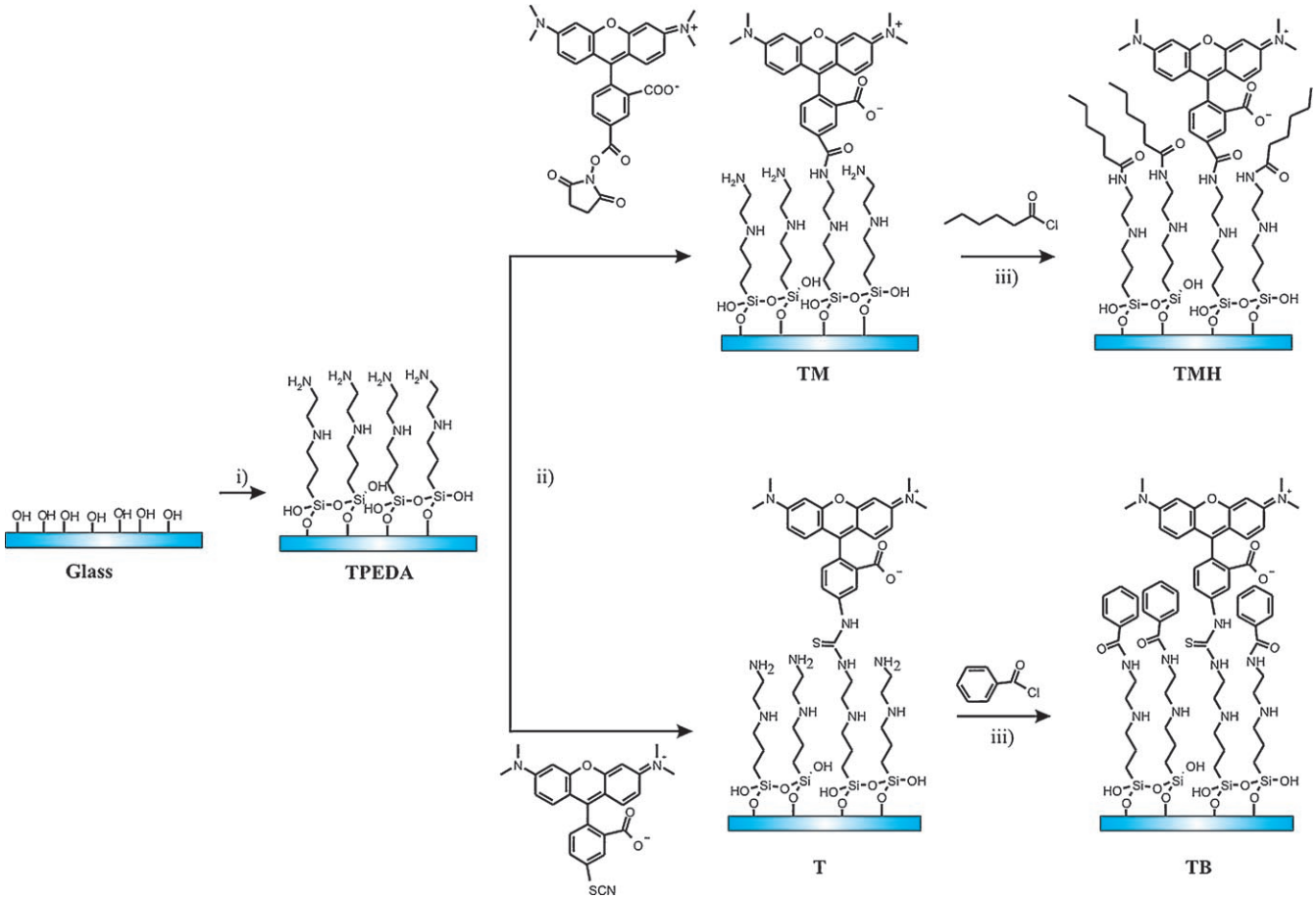

Figure 7. Synthetic scheme for fabrication of TMH and TB SAMs. i) *N*-[3-(trimethoxysilyl)propyl]ethylenediamine, toluene, *RT*, 3.5 h; ii) TAMRA or TRITC to yield TM and T SAMs, respectively, acetonitrile, *RT*, 4 h; iii) Hexanoyl chloride or benzyl chloride to afford TMH and TB layers, respectively, chloroform, *RT*, 16 h.

For the cross-shaped pattern, the AFM was also operated to write in contact mode. The cross was written by scanning over an area of 60×1.87 μm for each rectangle at a speed of 1 Hz (120 μm s^{-1}). Each line was scanned for 30 min. The relative humidity of the air was 32–34%, and the temperature in the room 25–26 °C. CLSM images of the TMH and TB surfaces patterned with metal ions by DPN were acquired on a Carl Zeiss LSM 510 microscope equipped with an argon laser module (Carl Zeiss Inc., Thornwood, NY) by using a 40× NA 0.75 objective. Samples were excited at 543 nm. The emitted fluorescence was collected with an R6357 photomultiplier tube. All confocal microscopy images were acquired in air. The maximum friction voltage of Figure 3a is 0.3 V.

A custom-built atomic force fluorescence microscope (AFFM) was used to perform dip-pen nanolithography and to immediately observe patterning results without changing to another instrument. A detailed description of the AFFM has been presented by Kassies et al.[33] Commercial Si_3N_4 AFM cantilevers with nominal spring constant of 0.05 N m^{-1} were used. Immediately before a DPN experiment, cantilevers were rinsed rigorously with ethanol and dried under an N_2 stream very gently. After cleaning, the cantilevers were exposed to UV light for 30 min to break down contaminants and make the cantilever surface more hydrophilic. Cleaned cantilevers were immersed in 10^{-1} M ethanol solutions of the perchlorate salts of Ca^{2+} ions for 5 min and then dried in air. The Ca^{2+}-coated cantilever was immediately mounted on the AFM head to carry out DPN experiments on TMH SAMs in contact mode with or without a humid air stream at a temperature between 20 and 23 °C. The humid air was created by passing dry nitrogen through two bottles of milliQ water followed by a bottle containing glass beads (∅5 mm) to create moist air near the AFM tip.[43] This simple humidity generator was used only when the environmental humidity was very low. By using the humidity generator, the RH value near the cantilever can be raised to approximately 50%. The force applied to the substrate by the AFM tip was kept between 10 and 30 nN in all experiments to avoid destruction of the fluorescent SAMs. The trace of the scanned cantilever was consistent with the re-trace. The 15×15 μm square-shaped patterns were written twice with a scan rate of 28 μm s^{-1}. Furthermore, 18 μm long fluorescent lines were fabricated with defined number of scans (15 scans) or controlled scan rate (1.8 μm s^{-1}). During the writing period, the fluorescence excitation light was switched off to prevent photobleaching of the samples. Immediately after DPN, the patterned substrate was excited with 488 nm argon laser light, and the fluorescence emission was recorded by an avalanche photodiode (APD; SPCM-AQR-14, Perkin-Elmer Optoelectronics). The acquired fluorescent images were analyzed by the commercial software SPIP (Image Metrology, Version 4.4.3.0).

Acknowledgements

We thank Martijn van Raaij for his help at the beginning of the AFFM experiments and Dr. Martine Cantuel for her kind discussion. This work was supported by the Royal Netherlands Academy of Arts and Sciences (KNAW), the MESA Institute for Nanotechnology, and NanoNed.

Keywords: atomic force microscopy · fluorescence · monolayers · nanotechnology · sensors

[1] G. M. Whitesides, *Small* **2005**, *1*, 172–179.
[2] D. S. Ginger, H. Zhang, C. A. Mirkin, *Angew. Chem.* **2004**, *116*, 30–46; *Angew. Chem. Int. Ed.* **2004**, *43*, 30–45.
[3] K. Salaita, Y. H. Wang, C. A. Mirkin, *Nat. Nanotechnol.* **2007**, *2*, 145–155.
[4] A. A. Tseng, A. Notargiacomo, T. P. Chen, *J. Vac. Sci. Technol. B* **2005**, *23*, 877–894.
[5] J. H. Lim, C. A. Mirkin, *Adv. Mater.* **2002**, *14*, 1474–1477.
[6] Y. Li, B. W. Maynor, J. Liu, *J. Am. Chem. Soc.* **2001**, *123*, 2105–2106.
[7] S. H. Hong, J. Zhu, C. A. Mirkin, *Science* **1999**, *286*, 523–525.
[8] M. Zhang, D. Bullen, S. W. Chung, S. Hong, K. S. Ryu, Z. F. Fan, C. A. Mirkin, C. Liu, *Nanotechnology* **2002**, *13*, 212–217.
[9] S. Deladi, N. R. Tas, J. W. Berenschot, G. J. M. Krijnen, M. J. De Boer, J. H. De Boer, M. Peter, M. C. Elwenspoek, *Appl. Phys. Lett.* **2004**, *85*, 5361–5363.
[10] Multiple inking is possible by using microfluidic networks over the PDMS stamps. A. Papra, A. Bernard, D. Juncker, N. B. Larsen, B. Michel, E. Delamarche, *Langmuir* **2001**, *17*, 4090–4095.
[11] P. Vettiger, M. Despont, U. Drechsler, U. Durig, W. Haberle, M. I. Lutwyche, H. E. Rothuizen, R. Stutz, R. Widmer, G. K. Binnig, *IBM J. Res. Dev.* **2000**, *44*, 323–340.
[12] R. D. Piner, J. Zhu, F. Xu, S. H. Hong, C. A. Mirkin, *Science* **1999**, *283*, 661–663.
[13] X. G. Liu, L. Fu, S. H. Hong, V. P. Dravid, C. A. Mirkin, *Adv. Mater.* **2002**, *14*, 231–234.
[14] S. W. Lee, B. K. Oh, R. G. Sanedrin, K. Salaita, T. Fujigaya, C. A. Mirkin, *Adv. Mater.* **2006**, *18*, 1133–1336.
[15] L. M. Demers, D. S. Ginger, S. J. Park, Z. Li, S. W. Chung, C. A. Mirkin, *Science* **2002**, *296*, 1836–1838.
[16] M. Su, X. G. Liu, S. Y. Li, V. P. Dravid, C. A. Mirkin, *J. Am. Chem. Soc.* **2002**, *124*, 1560–1561.
[17] M. Su, V. P. Dravid, *Appl. Phys. Lett.* **2002**, *80*, 4434–4436.
[18] A. Mulder, S. Onclin, M. Peter, J. P. Hoogenboom, H. Beijleveld, J. Ter Maat, M. F. García-Parajǒ, B. J. Ravoo, J. Huskens, N. F. Van Hulst, D. N. Reinhoudt, *Small* **2005**, *1*, 242–253.
[19] D. J. Pena, M. P. Raphael, J. M. Byers, *Langmuir* **2003**, *19*, 9028–9032.
[20] H. Jung, R. Kulkarni, C. P. Collier, *J. Am. Chem. Soc.* **2003**, *125*, 12096–12097.
[21] R. Mckendry, W. T. S. Huck, B. Weeks, M. Florini, C. Abell, T. Rayment, *Nano Lett.* **2002**, *2*, 713–716.
[22] M. Yang, P. E. Sheehan, W. P. King, L. J. Whitman, *J. Am. Chem. Soc.* **2006**, *128*, 6774–6775.
[23] L. A. Porter, H. C. Choi, J. M. Schmeltzer, A. E. Ribbe, L. C. C. Elliott, J. M. Buriak, *Nano Lett.* **2002**, *2*, 1369–1372.
[24] B. W. Maynor, Y. Li, J. Liu, *Langmuir* **2001**, *17*, 2575–2578.
[25] R. A. Vega, D. Maspoch, C. K. F. Shen, J. J. Kakkassery, B. J. Chen, R. A. Lamb, C. A. Mirkin, *ChemBioChem* **2006**, *7*, 1653–1657.
[26] M. J. W. Ludden, A. Mulder, R. Tampé, D. N. Reinhoudt, J. Huskens, *Angew. Chem.* **2007**, *119*, 4182–4185; *Angew. Chem. Int. Ed.* **2007**, *46*, 4104–4107.
[27] E. Delamarche, J. Vichiconti, S. A. Hall, M. Geissler, W. Graham, B. Michel, R. Nunes, *Langmuir* **2003**, *19*, 6567–6569.
[28] X. G. Liu, Y. Zhang, D. K. Goswami, J. S. Okasinski, K. Salaita, P. Sun, M. J. Bedzyk, C. A. Mirkin, *Science* **2005**, *307*, 1763–1766.
[29] L. Basabe-Desmonts, J. Beld, R. S. Zimmerman, J. Hernando, P. Mela, M. F. G. García-Parajó, N. F. Van Hulst, A. Van Den Berg, D. N. Reinhoudt, M. Crego-Calama, *J. Am. Chem. Soc.* **2004**, *126*, 7293–7299.
[30] L. Basabe-Desmonts, D. N. Reinhoudt, M. Crego-Calama, *Adv. Mater.* **2006**, *18*, 1028–1032.
[31] R. S. Zimmerman, L. Basabe-Desmonts, F. Van der Baan, D. N. Reinhoudt, M. Crego-Calama, *J. Mater. Chem.* **2005**, *15*, 2772–2777.
[32] M. Crego-Calama, D. N. Reinhoudt, *Adv. Mater.* **2001**, *13*, 1171–1174.
[33] R. Kassies, K. O. Van Der Werf, A. Lenferink, C. N. Hunter, J. D. Olsen, V. Subramaniam, C. Otto, *J. Microsc.* **2005**, *217*, 109–116.
[34] In the course of our experiments, a strong relation between ink transfer and relative humidity (RH) in the environment was observed. The RH was controlled by using a simple humidity generator when the ambient air was too dry, and experiments were performed at a humidity around 50%. A more precise RH generator is being developed.
[35] M. Su, Z. X. Pan, V. P. Dravid, T. Thundat, *Langmuir* **2005**, *21*, 10902–10906.
[36] J. Haaheim, R. Eby, M. Nelson, J. Fragala, B. Rosner, H. Zhang, G. Athas, *Ultramicroscopy* **2005**, *103*, 117–132.

[37] S. Deladi, N. R. Tas, J. W. Berenschot, G. J. M. Krijnen, M. J. de Boer, J. H. de Boer, M. Peter, M. C. Elwenspoek, *Appl. Phys. Lett.* **2004**, *85*, 5361–5363.
[38] A. P. Fang, E. Dujardin, T. Ondarcuhu, *Nano Lett.* **2006**, *6*, 2368–2374.
[39] K. H. Kim, N. Moldovan, H. D. Espinosa, *Small* **2005**, *1*, 632–635.
[40] K. H. Kim, R. G. Sanedrin, A. M. Ho, S. W. Lee, N. Moldovan, C. A. Mirkin, H. D. Espinosa, *Adv. Mater.* **2008**, *20*, 330–334.
[41] N. Moldovan, K. H. Kim, H. D. Espinosa, *J. Microelectromech. Syst.* **2006**, *15*, 204–213.
[42] J. Y. Jang, S. H. Hong, G. C. Schatz, M. A. Ratner, *J. Chem. Phys.* **2001**, *115*, 2721–2729.
[43] J. M. Maxwell, M. G. Huson, *Rev. Sci. Instrum.* **2002**, *73*, 3520–3524.

Received: December 21, 2007
Revised: May 15, 2008
Published online on July 21, 2008

